A Mutation in the Signal Recognition Particle 7S RNA of the Yeast *Yarrowia lipolytica* Preferentially Affects Synthesis of the Alkaline Extracellular Protease: *In vivo* Evidence for Translational Arrest

Debbie S. Yaver, Sam Matoba,* and David M. Ogrydziak*

Department of Microbiology, University of California, Davis, California 95616; and *Institute of Marine Resources, University of California, Davis, California 95616

Abstract. Replacement of the signal recognition particle (SRP) 7S gene (*SCR1*) on a replicating plasmid with *scr1-1* (G to A at 129 and A to T at 131 in the consensus sequence -GNAR- in the loop of domain III) resulted in temperature sensitivity for growth of cells in which both chromosomal SRP 7S RNA genes were deleted. Pulse-chase immunoprecipitation experiments were done after a shift to non-permissive temperature using the major secreted protein the alkaline extracellular protease (AEP) as a reporter molecule. No untranslocated AEP precursor was detected in a strain with *scr1-1* on a plasmid, but the amount of the largest AEP precursor (55 kD) immunoprecipitated as a percentage of total protein synthesized was reduced 68% compared to an isogenic strain with *SCR1* on the plasmid. The possibility that an untranslocated precursor was synthesized but not detected because of instability was largely eliminated by detection of a 53-kD untranslocated precursor of a mutated AEP (P17M; methionine replaced proline in the second position of the pro-peptide) which chased to the 55-kD translocated AEP precursor. Thus, SRP has a role in the biosynthesis of AEP. Possibly, the *scr1-1* mutation does not affect signal recognition or translational arrest but instead results in maintenance of translational arrest of AEP synthesis. The results also suggest that AEP can be translocated in vivo either co-translationally in which SRP is at least involved in biosynthesis or posttranslationally without SRP involvement.

In higher eukaryotes, evidence suggests that the signal recognition particle (SRP)[1] is essential for protein translocation across the ER membrane. SRP is a soluble 11S ribonucleoprotein composed of six polypeptides (72, 68, 54, 19, 14, and 9 kD) and a single 7S RNA of 300 nucleotides (66, 74). From the study of in vitro systems, a model has been proposed in which SRP functions as an adapter between the translational machinery in the cytoplasm and the translocational machinery in the ER membrane (49, 66, 74). The functions of individual SRP proteins have been elucidated by the study of "mutant" SRPs reconstituted in vitro (63, 65). Three functions of SRP have been identified: signal recognition, elongation arrest, and translocation promotion (66). Translation of mRNAs coding for secretory proteins begins on free ribosomes in the cytoplasm. When the polypeptide chain has elongated sufficiently, SRP binds the signal sequence/ribosome complex. This interaction results in arrest or pausing of translation (74, 78). The SRP/ribosome complex is then targeted to the SRP receptor, an ER integral membrane protein. This results in the release of SRP and translational arrest, and the polypeptide is then co-translationally translocated into the ER. During or shortly after translocation, signal peptide cleavage and core glycosylation occur. Besides a role as a scaffold for binding SRP proteins (73), functional roles for SRP 7S RNA in elongation arrest and in interaction with the SRP receptor have been proposed (36, 63, 81). Recently, it has been shown that SRP 7S RNA undergoes conformational changes which possibly are a necessary component for movement through the SRP cycle (3).

The study of the in vivo functions of SRP was made possible by the isolation of SRP homologues and SRP 7S RNA genes in two genetically tractable organisms, *Yarrowia lipolytica* (30, 46) and *Schizosaccharomyces pombe* (12, 46, 51). The yeast RNAs resemble higher eukaryotic 7S RNA with respect to size, transcriptional start signals, 5′ end structures, potential secondary structures, and binding under stringent conditions to mammalian SRP proteins. *S. pombe* contains a single essential SRP 7S RNA (12, 51). Mutations in a conserved tetranucleotide loop in domain IV demonstrated it is important for function; several of the mutations resulted in osmotic sensitivity at higher temperatures (37).

Homologues to Srp54p have been isolated from *Saccharomyces cerevisiae* and *S. pombe* (1, 26). Antibodies against Srp54p from *S. pombe* coprecipitate the *S. pombe* 7S RNA, and antibodies against Srp54p from *S. cerevisiae* coprecipitate *S. cerevisiae SCR1* RNA (519 nucleotides)

1. *Abbreviations used in this paper*: AEP, alkaline extracellular protease; SRP, signal recognition particle.

(Hann, B. C., and P. Walter. 1990. *J. Cell Biol.* 111:386*a*). Deletion of 252 nucleotides from the *SCR1* coding region results in sick but viable cells (22). Recent studies in *E. coli*, although controversial (7, 8, 13, 48), suggest that a ribonucleoprotein containing the 4.5S RNA has SRP-like properties (47, 52) and that protein secretion can occur by posttranslational and SRP-like homologue mediated co-translational pathways (47, 50, 52).

In this study we isolated a temperature sensitive mutation in one of the genes *(SCR1)* coding for the *Y. lipolytica* SRP 7S RNA. *Y. lipolytica* is a dimorphic, heterothallic yeast which is quite different from *S. cerevisiae* (5) and *S. pombe*. *Y. lipolytica* contains two functional SRP 7S RNA genes: *SCR1* and *SCR2* (31). Disruption of either gene alone has no obvious effect on growth or secretion, but disruption of both genes is lethal (31). *Y. lipolytica* secretes significant levels of several hydrolytic enzymes, and it produces an alkaline extracellular protease (AEP) at levels of 1 to 2% of total cell protein (40, 43). AEP processing involves several intracellular precursors; the largest and earliest precursor detected in pulse-chase immunoprecipitation experiments is a 55-kD translocated polypeptide which lacks the signal peptide (21, unpublished data) but contains 2 kD of N-linked carbohydrate (39, 40). The next largest AEP precursor is a 52-kD polypeptide which results from dipeptidyl aminopeptidase processing (39). The major processing pathway is from the 55- to the 52-kD precursor and then to the 32-kD mature AEP (40). In wild type strains, even with short labeling times, no untranslocated AEP precursor is detected suggesting that translocation is co-translational. If the *scr1-1* mutation affected signal peptide recognition then one would expect untranslocated AEP precursors to accumulate, but instead we found that this mutation had a preferential effect on biosynthesis of AEP. One possibility is that the *scr1-1* mutation does not affect the signal recognition and translational arrest functions of SRP but that translational arrest is maintained.

In higher eukaryotes, translocation is generally thought to be SRP mediated and co-translational (74). In vitro SRP-independent posttranslational translocation across dog pancreas microsomal membranes has recently been demonstrated (61). In *S. cerevisiae*, there are several proteins for which posttranslational translocation has been demonstrated in vivo (2, 10, 20, 38, 41, 57, 67, 70) or in vitro (27, 28, 55, 70, 75). We show that a mutation in the pro-region of AEP results in its efficient (but slow) posttranslational translocation. Therefore, it appears that AEP can use both posttranslational and co-translational (with SRP at least involved in AEP biosynthesis) translocation pathways.

Materials and Methods

Materials

Protosol and Econofluor were obtained from Dupont, New England Nuclear Research Products (Boston, MA). L-[4,5-^{3}H]leucine and L-[^{35}S]methionine (>800 Ci/mmol) were obtained from Amersham Corp. (Arlington Heights, IL). PMSF and 4-hydroxymercuribenzoic acid were from Calbiochem-Behring Corp. (San Diego, CA). Casein (Hammersten) was purchased from ICN Pharmaceuticals Inc. (Irvine, CA), and polypropylene glycol (2,000 molecular weight) was from Aldrich Chemical Co., Inc. (Milwaukee, WI). Benzamide, leupeptin, DMSO, concanavalin A-Sepharose 4B, methyl-α-D-mannopyranoside, and Triton X-100 were from Sigma Chemical Co. (St. Louis, MO). EDTA was from Fisher Scientific, (Pittsburgh, PA). Restriction enzymes, other DNA modifying enzymes, the Random-primed DNA Labeling Kit, and proteinase K were purchased from Boehringer-Mannheim Biochemicals (Indianapolis, IN), New England Biolabs (Beverley, MA) and Amersham (Arlington Heights, IL). Protein A-Sepharose 4 Fast Flow was purchased from Pharmacia Fine Chemicals (Piscataway, NJ). AEP antiserum was prepared as described previously (40). The drug 5-fluoroorotic acid *(5-FOA)* was obtained from SCM (Specialty Chemicals, Gainesville, FL).

Growth Media

Complete medium was YEPD, and minimal medium was YNB-glucose (62). Cultures were maintained on YM (40). YM$^+$ was YM supplemented with uracil (33 mg/ml), leucine (150 mg/ml), and hypoxanthine (100 mg/ml). Cultures were grown in YPDC (1% yeast extract, 1% bactopeptone [Difco Laboratories Inc., Detroit, MI], 1% dextrose, 50 mM sodium citrate, pH 4.0) for transformation (79). For Lys$^-$ strains, lysine, or glutamic acid at a final concentration of 0.1% was used instead of ammonium sulfate in minimal medium since Lys$^-$ strains do not grow on ammonium sulfate as the nitrogen source. GPP* medium (40) was used for the growth of cultures for labeling experiments; it contained 1.0% glycerol, 0.24% Proteose peptone (Difco Laboratories Inc.), 0.17% yeast nitrogen base without amino acids or ammonium sulfate (Difco Laboratories Inc.), 40 mM phosphate buffer pH 6.8, and 0.003% adenine. GC medium is GPP* with 0.4 gm of casein per liter substituted for Proteose peptone. The 5-FOA-selective medium was prepared as described by Boeke et al. (11) except the pH was adjusted to 7.0.

Plasmids and Strains

For DNA manipulations *E. coli* strains HB101 or JM105 were used (59). The *E. coli* strains used for site-directed mutagenesis were MV1190 and CJ236 (24).

The *Y. lipolytica* haploid needed for the plasmid shuffle was constructed by first mating DX606-3D *scr1::ADE1 ura3 leu2 pro1* with 21501-4 *lys5 leu2 ade1 xpr2* (provided by C. Gaillardin, INRA, Thiverval-Grignon, France) using standard protocols (6, 44). One of the segregants from this cross DX621-1 *scr1::ADE1 leu2 lys5 ura3 xpr2* was mated with DX588-1B *ade1 leu2 trp1 ura3*. The diploid was sporulated and random spore analysis was done. Three segregants with the desired phenotype of *scr1::ADE1 leu2 lys5 ura3* were analyzed by Southern blotting to confirm the presence of the *scr1::ADE1* disruption. One of the segregants DX642-3 *scr1::ADE1 leu2 lys5 ura3* was transformed with pIMR59 which contained the *SCR1* and *URA3* genes and *ARS18* an autonomously replicating sequence (provided by P. Fournier, INRA, Thiverval-Grignon, France). Ura$^+$ transformants were selected. After confirming that one of the Ura$^+$ transformants contained the plasmid, the *SCR2* chromosomal locus was disrupted with a *scr2::LYS5* allele (58). The *SCR2* disruption was constructed by digesting pINA400 (provided by C. Gaillardin) with *Sal*I to remove the *URA3* gene. The plasmid pINA400 is a pBluescript plasmid containing the 3.2-kb *HindIII-XhoI SCR2* fragment from which a 570-bp *DraI-EcoRV* fragment, which includes the entire coding region of *SCR2*, had been deleted and into which the *URA3* gene had been inserted to construct the *scr2::URA3* disruption (31). The *Sal*I-digested pINA400 was treated with Klenow fragment to create blunt ends and with calf intestinal alkaline phosphatase to prevent self-ligation and ligated to the 4.4-kb *Sph*I-*Bgl*II *LYS5* fragment which had been blunt-ended using T4 DNA polymerase. The resulting recombinant plasmid pIMR54 was digested with *Apa*I and *Not*I to target integration to the *SCR2* locus (58). The DX642-3 strain containing pIMR59 was transformed and Lys$^+$ transformants were selected. The presence of the *scr2::LYS5* disruption was confirmed by Southern analysis. This strain was used for the isolation of conditional mutations of *SCR1* and provided the isogenic background used for the in vivo analysis of the effects of *scr1-1* on protein secretion.

DY63 and DY66 were obtained by replacing pIMR59 in this strain with pIMR63 (*SCR1*) and pIMR66 (*scr1-1*), respectively. For the construction of pIMR63, pINA240 which contains the *ARS18* and *LEU2* fragments was digested with *Nde*I, blunt-ended, and religated to destroy the *Nde*I site to create pIMR62. A 2.5-kb *Bam*HI/*Apa*I fragment containing *SCR1* was isolated, and *Bam*HI linkers were added. The 2.5-kb *Bam*HI *SCR1* fragment was subcloned into pIMR62 to get pIMR63. To obtain pIMR66, a 560-bp *Nde*I/*Mlu*I*scr1-1* fragment was subcloned into pIMR63. For pIMR59, the *LEU2* fragment in pINA240 was replaced with the 1.7-kb *URA3 Sal*I fragment to give pIMR53, and the 2.5-kb *SCR1 Bam*HI piece described above was subcloned into pIMR53.

The glycosylation and NH_2-terminal sequencing studies of the P17M mutation were done in a strain derived from CX161-1B *ade1 A* (40). Details of the plasmid constructions for the deletions of *URA3* (400-bp *Eco*RV fragment) and *XPR2* (150-bp *Apa*I fragment) will be described elsewhere. These

deletions were incorporated sequentially into CX161-1B by a two-step gene replacement technique using 5-FOA selection (11). The P17M mutation was incorporated into the *ade1 URA3 XPR2* strain by transforming with pIMR118 cut at *MluI* in the *XPR2* promoter region, selecting Ura^+ transformants, and then selecting Ura^- Xpr^+ strains after growth on 5-FOA. Replacement of the *XPR2* deletion was confirmed by Southern analysis. The plasmid pIMR118 containing the P17M mutation was constructed by replacing a 1,655-bp *SphI/XbaI* fragment in pIMR101 with the *SphI/XbaI* fragment containing the mutation; pIMR101 contains a 2.76-kb *SphI/EcoRI XPR2* fragment and a 1.7-kb *SalI URA3* fragment in pBR322.

The P17M mutation was incorporated into DY63 and DY66 in two steps. Since these strains were Xpr^+, first the 150-bp *ApaI* fragment deletion in *XPR2* was incorporated by the two-step gene replacement using 5-FOA (11) to obtain an Xpr^- strain. Then the P17M mutation, which yields an Xpr^+ phenotype, was incorporated as described above for the *ade1 xpr2 ura3* strain.

In Vitro Mutagenesis

Site-directed mutagenesis was done using the Bio-Rad Muta-gene M13 in vitro mutagenesis kit and its detailed protocols and strains; the kit is based on methods described by Kunkel et al. (35). For the two base pair change mutation in *scrl-1*, the primer used was 5'-CGGTCTGAATTATCG-GCTTT-3'. For P17M, the oligonucleotide used was 5'-CGTTCTGGCCGC-TATGCTGGCCGCCCCTG-3' in which ATG replaces CCC coding for proline at position 17 in AEP.

Pulse–Chase Immunoprecipitation

Labeling, preparation of cell extracts with glass beads, and immunoprecipitation were done as described previously (40). Cells were grown in GPP* medium and resuspended in GC medium at a cell density of 1,000 Klett U (2×10^8 cells/ml). For experiments in which cells were shifted to 33°C for one or two hours, GPP* cultures were shifted to 33°C for 20 min or 1 h and 20 min, respectively. After harvesting, the cells were resuspended in prewarmed GC and incubated at 33°C for 40 min. After 40 min in GC, 250 mCi of L-[4,5-^{3}H]leucine (120–190 Ci/mmol) was added for every 6 ml of cells. Cells were labeled for 45 s, and chased with 3,000-fold excess of cold L-leucine. Cell extracts were prepared and immunoprecipitated and supernatant proteins TCA precipitated as described previously (40) with the following modifications: (*a*) clarified cell extracts were adjusted to 4% Triton X-100 before the addition of antiserum; (*b*) 50 μl of washed, packed protein A-Sepharose 4 Fast Flow was added to the antiserum and cell extract mixture; and (*c*) TCA-precipitated supernatant samples were neutralized with 1 M Tris instead of NaOH. Total incorporation of label was measured at selected post-chase time points by scintillation counting of boiled TCA precipitates from two 100 μl samples of labeled cell suspension (40).

Endoglycosidase H Digestion

Endoglycosidase H (endo H) from ICN (Irvine, CA) was prepared as described by the supplier. It was dissolved in 230 μl of 50 mM sodium citrate, pH 5.5, 0.1% SDS, and 5 mM sodium azide to 1 mU/ml. This stock was stored at −80°C and was diluted to 0.2 mU/μl before use.

Pulse-chase immunoprecipitation samples were ethanol precipitated; 50 or 100 μl of non-reduced sample was added to 1 ml of 100% ethanol and incubated overnight at −20°C. After centrifugation at 12,000 rpm at 4°C for 30 min, the pellet was washed with 70% ethanol and dried. The pellet was resuspended in 25 μl of 500 mM sodium citrate, pH 5.5, 0.1% SDS, 2 mM PMSF. To the sample, 5 μl of dilute endo H (0.2 mU/μl) was added. The digestion was incubated at 37°C over night, an additional 5 μl of dilute endo H was added, and the incubation was continued at 37°C for another 6 h. To terminate the reaction, Laemmli loading buffer (4×) (39) was added, and the mixture was boiled for 5 min.

PAGE and Fluorography

Proteins were analyzed by electrophoresis in 10 to 15% linear gradient polyacrylamide gels (40). For immunoprecipitates, 25 μl of sample, equivalent to 0.375 ml of suspended cells, was applied per lane. Extracellular proteins precipitated by TCA were dissolved in 250 μl of Laemmli buffer, and 25 μl, equivalent to 0.3 ml of suspended cells, was loaded per lane.

After electrophoresis, gels were stained with Coomassie brilliant blue and destained in 10% methanol, 15% acetic acid. The gels were treated with DMSO and the scintillator 2,5-diphenyloxale. The treated gels were dried and exposed to preflashed Kodak X-Omat AR film and stored at −80°C.

Gel slices were rehydrated in 50 μl of water and solubilized by shaking overnight at 37°C in 10 ml of Econofluor-Protosol mixture (95:5) in glass vials (40).

Glycoprotein Precipitation with ConA

Cells were grown and labeled as described previously except the labeling period was extended to two minutes. Samples were processed as described previously. Of the 600 ml of clarified extract, 585 μl was immunoprecipitated with AEP antiserum. 15 μl of the cell extract was diluted with 135 μl of ConA reaction buffer (0.5 M NaCl, 20 mM Tris, pH 7.4, 2% Triton X-100) (19), and 25 μl of packed Con A–Sepharose 4B was added followed by incubation at 4°C for 3 h on a rocking platform. Con A–Sepharose beads were sedimented by centrifugation. The unbound supernatant was removed and saved. The beads were washed three times with 1 ml of Con A reaction buffer. Bound glycoproteins were eluted with 200 μl of 300 mM methyl-α-D-mannopyranoside, 2 mM PMSF, 0.5 M NaCl, 20 mM Tris, pH 7.4, 2% Triton X-100 at room temperature for 1 h with shaking. After the beads were pelleted, the supernatant containing eluted glycoproteins was removed. The ratio of bound counts to total counts was determined by scintillation counting of the bound and unbound fractions.

RNA Analysis

Total RNA, prepared as described by Davidow et al. (18), was electrophoresed on an agarose gel containing formaldehyde (59). The RNA was transferred to Zeta probe nylon membrane (Bio-Rad Laboratories, Richmond, CA) according to the manufacturer's instructions. Probes were prepared by random primed DNA labeling.

DNA Sequencing

Single (68) and double stranded (15) DNA sequencing was done by the dideoxy method (60) using the Sequenase kit (United States Biochemical, Cleveland, OH) and [^{35}S]dATP (9).

Radiosequencing

Radiolabeled cell extracts were prepared as described previously with the following modifications: cells were kept at 23°C during growth and after transfer to GC medium. After 30 min in GC medium, 20 ml of cells were double labeled for 100 s with 1 mCi of L-[^{35}S]methionine and 1 mCi of L-[4,5-^{3}H]leucine and chased with 3,000-fold excess of unlabeled methionine and leucine. Samples were taken as soon as possible and 10 min after the addition of the chase for the 53- and the 55-kD AEP precursor samples, respectively. The immunoprecipitates were run on a 10–15% SDS-PAGE gel for which the precautions recommended by Hunkapillar et al. (33) were taken. The labeled bands were electrophoretically transferred to Immobilon PVDF membrane (Millipore, Bedford, MA) (69). The membrane was extensively washed, blotted dry, and exposed to X-ray film to locate the bands. The bands were cut out, extensively washed, and subjected to automated Edman degradation in an Applied Biosystems 470A gas phase sequencer. The [^{35}S]methionine and [^{3}H]leucine counts in each cycle were determined by double-channel counting with a scintillation counter (model 7500; Beckman Instruments, Inc., Palo Alto, CA).

Protease Protection

The protease protection experiments were based on protocols published for *S. cerevisiae* (56) and *Y. lipolytica* (21). Cell labeling and the chase were done as in a standard pulse-chase immunoprecipitation experiment except that labeling was for 60 s. A 12-ml sample was taken 1.5 min after addition of the chase and added to 4.6 g of crushed ice containing sufficient sodium azide, leucine, and PMSF to give final concentrations of 10, 2.5, and 2 mM, respectively. Cells were incubated for 15 min at 30°C in sodium thioglycolate (30 mg/ml), 50 mM Tris-HCl (pH 9.1), and 0.8 M KCl. Cells were then incubated for 25 min at 30°C in JD buffer (1 M KCl, 20 mM MES, pH 6.0) containing 4 mg/ml of a lytic enzyme (obtained from J. DeZeeuw, Pfizer, Inc., Groton, CT) prepared from *Trichoderma harzianum* and ~0.2 mg/ml lyticase (No. L5263; Sigma Chemical Co.). Over 90% of the cells were spheroplasts after this incubation. The cells were washed three times with JD buffer and resuspended in 2 ml of homogenization buffer (0.3 M mannitol, 100 mM KCl, 1 mM EDTA, 50 mM Tris-HCl, pH 7.5) (56) containing an inhibitor cocktail to give final concentrations of 2 mM EDTA, 2 mM PMSF, 1 mM benzamide, 1 μg/ml leupeptin, and 50 μM 4-hydroxymercuribenzoic acid. Spheroplasts were lysed with 10 strokes by hand in a 10 ml Potter-Elvehjem tissue grinder (No. 358039; Wheaton Scientific, Millville,

NJ) and centrifuged for 5 minutes at 900 *g* (21). 6 ml of supernatant liquid was divided into four equal portions. In some samples, Triton X-100 and/or proteinase K were added to final concentrations of 0.4% and 0.5 mg/ml, respectively. The samples were incubated for 1 h at 0°C, TCA added to 10% (vol/vol), and after several hours incubation on ice the precipitate was washed with cold acetone and dried in the Speed Vac (Savant Instruments, Inc., Farmingdale, NY). To each sample, 200 μl of 50 mM, Tris-HCl (pH 6.8), 1 mM $MgCl_2$, 1 mM $CaCl_2$, 1 mM leucine was added. The solutions were made up to 1% SDS and 2 mM PMSF, vortexed, and incubated at room temperature for 10 min. Then Triton X-100 was added to 4% final concentration, the antibody added, and the standard immunoprecipitation protocol followed (40).

Results

Isolation of Conditional Alleles of SCR1

To begin elucidating the in vivo functions of the SRP 7S RNA, we isolated a conditional mutation in *SCR1* by site-directed mutagenesis. The mutation was designed based on the consensus sequence -GNAR- present in the stem-loop of domain III of all sequenced 7SL RNAs (14). The mutant allele *scr1-1* contained two base changes (G to A at 129 and A to T at 131) (Fig. 1), and it was shown to result in temperature-sensitive growth using a plasmid shuffle (11). A haploid in which both *SCR1* and *SCR2* chromosomal loci were disrupted and in which the *SCR1* and *URA3* genes were carried on an autonomously replicating plasmid (pIMR59) was transformed with an autonomously replicating plasmid carrying *scr1-1* and *LEU2* (pIMR66). Leu$^+$ transformants were selected, and plated on medium containing 5-FOA which inhibits growth of URA3$^+$ cells. A strain [DY66 (*scr1-1*)] carrying *scr1-1* on the *LEU2* plasmid grew on 5-FOA at 14 and 23°C but not at 33°C. The *scr1-1* plasmid was rescued from the strain and rescreened in the plasmid shuffle which confirmed that the temperature-sensitive phenotype was linked to the plasmid. The 560-bp *NdeI*/*MluI* fragment of the rescued plasmid was sequenced to confirm that it contained the *scr1-1* allele.

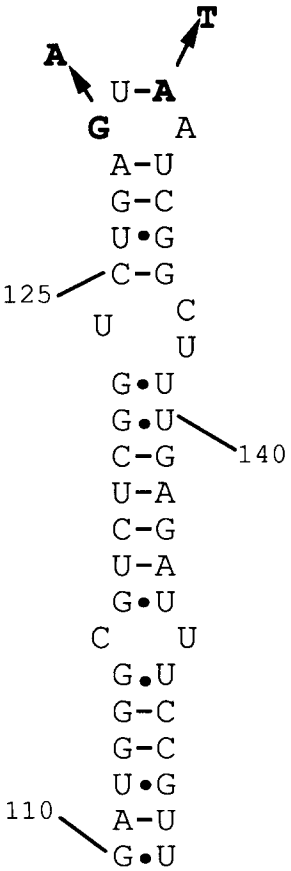

Figure 1. The *scr1-1* mutation. The figure depicts the stem loop structure in domain III of the *Y. lipolytica* SRP 7S RNA coded for by *SCR1* (adapted from Poritz et al., reference 46). For *scr1-1*, G at position 129 was changed to A and A at position 131 was changed to T.

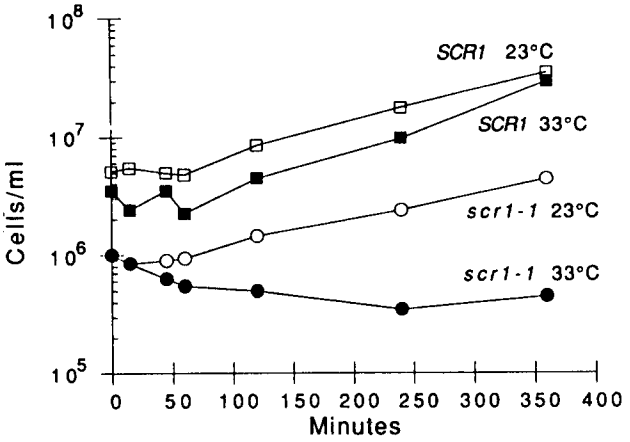

Figure 2. Cell viabilities of the DY63 (*SCR1*) and DY66 (*scr1-1*) isogenic strains following a shift to 33°C. Cultures were grown in YEPD at 23°C, and at zero time were split in half. Half was diluted twofold with prewarmed 33°C YEPD and shifted to 33°C. The other half was diluted twofold with 23°C YEPD and incubated at 23°C. Samples were plated on YM$^+$ and the plates incubated at 23°C to determine the number of cells (colony forming units) per ml.

The scr1-1 Allele at the Normal Chromosomal Locus Cannot Support Growth

We attempted to replace *SCR1* with the *scr1-1* allele at its normal chromosomal locus to construct a strain for in vivo studies of the effects of *scr1-1* on protein secretion. Integrating plasmids containing the *URA3* gene and either the *SCR1* or *scr1-1* allele were digested to target integration to the *scr1::ADE1* locus of DY63 [Δ*SCR1*, Δ*SCR2*, pIMR63 (*LEU2*, *SCR1*)]. Ura$^+$ transformants were selected and grown in YEPD medium supplemented with leucine to allow for loss of pIMR63. In the Leu$^-$ derivatives obtained, the only copy of the 7S RNA gene present should be that integrated at *scr1::ADE1*. These Leu$^-$ strains were then grown on 5-FOA to select for a homologous recombination event which should leave either the original *scr1::ADE1* allele or the recently integrated *SCR1* or *scr1-1* alleles at the normal chromosomal locus.

For the *SCR1* integrant, a successful transplacement occurred which was confirmed by Southern analysis (data not shown). However, the *scr1-1* integrants were unable to lose the *SCR1 LEU2* plasmid (pIMR63) even after growth in YEPD supplemented with leucine at 23°C for ~48 generations. No loss of pIMR63 was seen among the more than 3,200 colonies scored in contrast to the >50% loss frequency seen for the *SCR1* integrants. Loss of pIMR63 in the *scr1-1* integrants was also tested at 18°C, and no Leu$^-$ colonies were found among the >4,000 scored indicating that the chromosomal *scr1-1* could not support growth even at this lower temperature. Perhaps, higher levels of *scr1-1* 7S RNA are

produced from an autonomously replicating plasmid (copy number of 2 to 3)((23) than from its chromosomal locus, and at 23°C these higher levels can compensate for the defect caused by the structural alteration of the *scrl-1* 7S RNA.

We next investigated how quickly cells were irreversibly inactivated during incubation at 33°C so that they could no longer recover and grow when transferred back to 23°C (Fig. 2). DY63 (*SCRI*) and DY66 (*scrl-1*) were grown at 23°C and split at time zero; half was shifted rapidly to 33°C, and the other half was kept at 23°C. Samples were taken and plated on YM^+ at 23°C. At least half the number of DY66 (*scrl-1*) cells originally present could recover and grow even after 6 h at the nonpermissive temperature.

The scrl-1 Allele Preferentially Affects the Levels of a Secretory Protein

The isogenic strains DY63 (*SCRI*) and DY66 (*scrl-1*) were examined in pulse-chase immunoprecipitation experiments to obtain in vivo evidence for SRP involvement in protein secretion. AEP, which can account for up to 2% of total cell protein (40, 43), was used as the reporter molecule. AEP posttranslational processing results in several intracellular precursors (40). The earliest and largest precursor detected in wild type cells is a 55-kD polypeptide which presumably has been translocated into the ER because it contains 2 kD of N-linked carbohydrate (40) and it lacks the signal peptide (21, unpublished data). Even with pulse-labeling times as short as 30 s, untranslocated AEP precursors are not found (data not shown), suggesting that translocation is co-translational.

Our original expectation was that an untranslocated AEP precursor might accumulate in DY66 (*scrl-1*) but not in DY63 (*SCRI*). This precursor should still retain the 15 amino acid signal peptide but it should lack the 2 kD of N-linked carbohydrate, thus it would be predicted to have a mobility on SDS-PAGE similar to that of the 55-kD precursor. For both DY63 (*SCRI*) and DY66 (*scrl-1*), the only precursors detected at early time points after the cells were shifted to 33°C after 1 h were about 55 kD. Treatment with endo H revealed that both precursors contained about 2 kD of N-linked carbohydrate strongly suggesting that they had been translocated across the ER membrane (Fig. 3). Thus, we obtained no evidence for an untranslocated AEP precursor in *scrl-1* cells, and data presented below suggests that we would have been able to detect such a precursor.

We did notice, however, that in DY66 (*scrl-1*) the amount of labeled 55-kD precursor immunoprecipitated at all timepoints examined was consistently reduced in comparison to the levels detected in DY63 (*SCRI*) (Fig. 4, *a* and *c*). These differences were much greater than the 12% decrease (average of five experiments) in total protein synthesis found for DY66 (*scrl-1*) versus DY63 (*SCRI*). To quantitate the amounts of the 55-kD precursor immunoprecipitated, bands containing the precursor were cut from the gel, rehydrated, and counted in a scintillation counter. The absolute values of counts in 55-kD AEP precursor/total counts incorporated × 100% varied considerably from experiment to experiment; however, the relative ratios of the value for DY66(*scrl-1*) divided by that for DY63(*SCRI*) were fairly consistent within an experiment. For the 0, 1.5, and 3 min time points the ratios were 0.37 ± 0.22 (n = 5), 0.32 ± 0.18 (n = 4), and 0.28 ± 0.10 (n = 5) (mean ± SD, n = number of determinations).

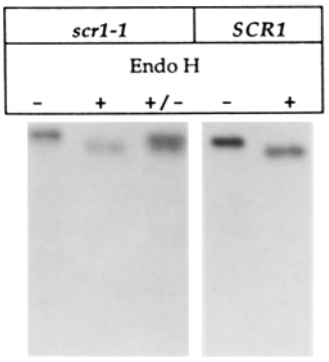

Figure 3. The 55-kD AEP precursors found in DY63 (*SCRI*) and DY66 (*scrl-1*) after 1 h at 33°C contain ~2 kD of N-linked carbohydrate. Immunoprecipitates from 0 time samples were treated with endo H and electrophoresed on a 10 to 15% linear gradient SDS-PAGE gel. The figure includes two sections of the same gel. For the three lanes on the left, the film was exposed for 75 d and for the two lanes on the right, 12 d. The lanes contain, from left to right, DY66 (*scrl-1*) immunoprecipitate, endo H digested DY66 (*scrl-1*) immunoprecipitate, endo H–digested and –undigested DY66 (*scrl-1*) immunoprecipitates combined, DY63 (*SCRI*) immunoprecipitate, and endo H–digested DY63 (*SCRI*) immunoprecipitate.

Therefore, ~68% reduction in the specific rate of AEP 55-kD precursor synthesis was observed with the *scrl-1* mutation. As would be predicted based on the above results, the levels of mature AEP secreted from DY66 (*scrl-1*) were also lower than from DY63 (*SCRI*) (Fig. 4 *b*), although the decrease was not as great as for the intracellular 55-kD AEP precursor (see Discussion).

After a 2 h shift to 33°C, a similar result of an approximate 75% reduction in AEP precursor levels in DY66 was also obtained. However, after a 15 min shift to 33°C, little or no effect on AEP biosynthesis was observed.

We examined the effects of the *scrl-1* mutation on other secreted proteins by measuring Con A bindable counts after either a 0, 1, or 2 h shift to 33°C. Con A binds mannose residues which are added in the secretory pathway (45) and to some extent in the cytoplasm and nucleus (29). Cells were labeled for 2 min followed by a chase. Samples were taken immediately, and intracellular extracts were incubated with Con A–Sepharose 4B. Total bound and unbound counts were measured, and the ratios of total bound counts to total counts (bound plus unbound) were calculated (Table I). After a 1 or 2 h shift to 33°C, total counts in glycoproteins were reduced on average by 27% in DY66 (*scrl-1*) as compared to DY63 (*SCRI*); whereas, when cells were grown and labeled at 23°C, the counts in the glycoproteins were comparable. The reduction of 27% in Con A bindable counts in the mutant strain is much less than the 68% reduction of the levels of AEP 55-kD precursor suggesting that the effect on most other glycoproteins traversing the secretory pathway is not as severe as for AEP.

To rule out two possible explanations for the lower levels of AEP precursors present in DY66 (*scrl-1*), *SCRI* RNA levels and AEP mRNA levels were compared in DY63 (*SCRI*) and DY66 (*scrl-1*) 1 h after a shift to 33°C. Total RNA from both strains was isolated after the temperature shift. Northern blots were probed with labeled *SCRI* and *XPR2* (AEP) gene fragments and with a probe for *rRNA* as a control for RNA recovery and loading. The levels of both AEP mRNA and 7S RNA present in the DY66 (*scrl-1*) were comparable to those seen in DY63 (*SCRI*) (data not shown). Therefore, lower levels of AEP mRNA or 7S RNA cannot account for the decrease in AEP precursors detected in the mutant *scrl-1* cells.

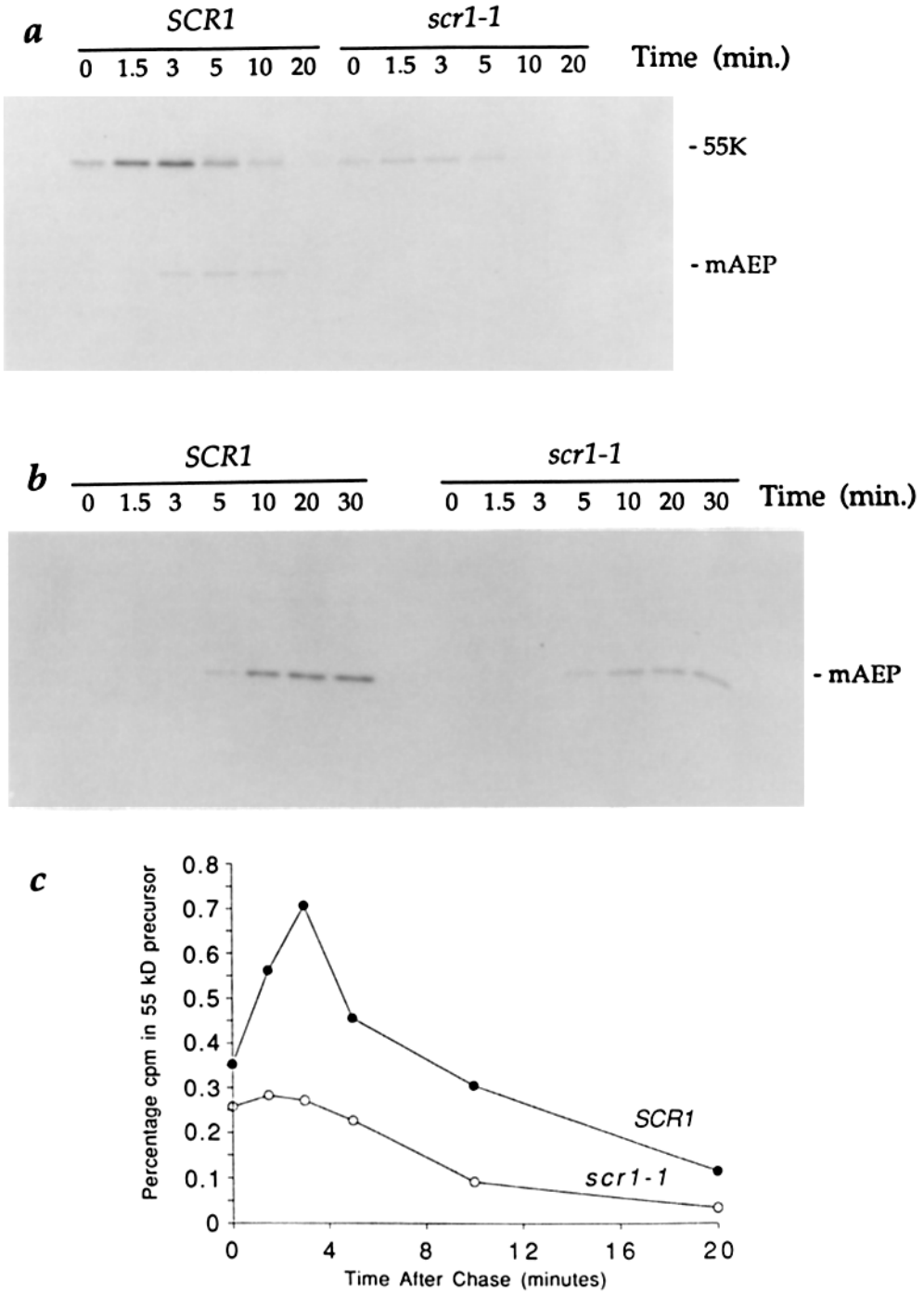

Figure 4. Levels of AEP precursors and secreted mature AEP are significantly lower in DY66 (*scr1-1*) than in the DY63 (*SCR1*) after 1 h at 33°C. (*a*) Immunoprecipitates from a pulse-chase experiment. Cells were shifted from 23° to 33°C, and after 1 h at 33°C they were labeled for 45 s with [^{3}H]leucine. Cell extracts were immunoprecipitated with AEP antisera and electrophoresed on a 10 to 15% linear gradient SDS-PAGE gel. (Lanes *1–6*) Immunoprecipitates of DY63 (*SCR1*) taken at the times indicated after the chase. (Lanes *7–12*) Immunoprecipitates of DY66 (*scr1-1*) taken at the times indicated after the chase. The positions of the 55-kD precursor and mature AEP are shown. The film was exposed for 3 d. Total counts incorporated in DY66 (*scr1-1*) were 77% of counts in DY63 (*SCR1*). (*b*) Extracellular samples. Total proteins from extracellular samples were precipitated with TCA and electrophoresed on a 10 to 15% linear gradient SDS-PAGE gel. (Lanes *1–7*) Extracellular samples from DY63 (*SCR1*). (Lanes *8–14*) Extracellular samples from DY66 (*scr1-1*). Times indicated are after the chase. The position of mature AEP is indicated. The film was exposed for 3 d. (*c*) Graph of counts in 55 kD AEP precursor/total counts incorporated × 100% versus time after addition of the chase for data shown in *a*.

Detection of an Untranslocated AEP Precursor Suggests That scr1-1 Affects Synthesis and Not Translocation of AEP: A Mutated AEP Can Be Translocated Posttranslationally

The decreased level of the 55-kD AEP precursor in DY66 (*scr1-1*) after a shift to 33°C could result from a decrease in AEP synthesis and/or from synthesis of an untranslocated AEP precursor which is short lived or extremely sensitive to endogenous proteases and therefore undetectable even with a very short pulse. The second possibility was largely eliminated by the fortuitous discovery of a mutated AEP (P17M) which is translocated posttranslationally. In P17M the proline in position 17, the second position in the 142 amino acid pro-peptide, was changed to methionine (see top of Fig. 7). The P17M allele of AEP was substituted for the wild type gene at its normal chromosomal locus, and the P17M strain was examined by pulse-chase immunoprecipitation experiments at either 23°C or after a 1 h shift to 33°C. The earliest detected AEP precursor was ~53 kD (Fig. 5 *a*), and the 53 kD precursor was completely chased to a 55-kD precursor (Fig. 5 *b*). Endo H digestions of the 53- and 55-kD precursors demonstrated that the 53-kD form is unglycosylated, and the 55-kD form contains 2 kD of N-linked carbohydrate (Fig. 6).

The endo H results suggest that the 53-kD AEP precursor

Table I. Total Glycoprotein Precipitated by Concanavalin A

Strain	Time at 33°C (h)	Total incorporation DY66/DY63 × 100%	CPM		Bound/Total*	(Bound/Total for DY66)/ (Bound/Total for DY63)
			Unbound	Bound		
DY66 (*scr1-1*)	0	106	1,277,000	26,800	0.031	103%
DY63 (*SCR1*)	0		1,616,000	32,600	0.030	
DY66 (*scr1-1*)	1	97	1,087,000	20,400	0.027	77%
DY63 (*SCR1*)	1		1,371,000	32,400	0.035	
DY66 (*scr1-1*)	1	99	1,060,000	23,200	0.021	77%
DY63 (*SCR1*)	1		808,500	23,100	0.028	
DY66 (*scr1-1*)	2	95	1,472,000	17,400	0.012	67%
DY63 (*SCR1*)	2		1,275,000	22,900	0.018	
DY66 (*scr1-1*)	2	119	731,000	38,200	0.050	70%
DY63 (*SCR1*)	2		702,500	52,300	0.069	

* CPM bound to ConA divided by CPM bound plus CPM unbound.

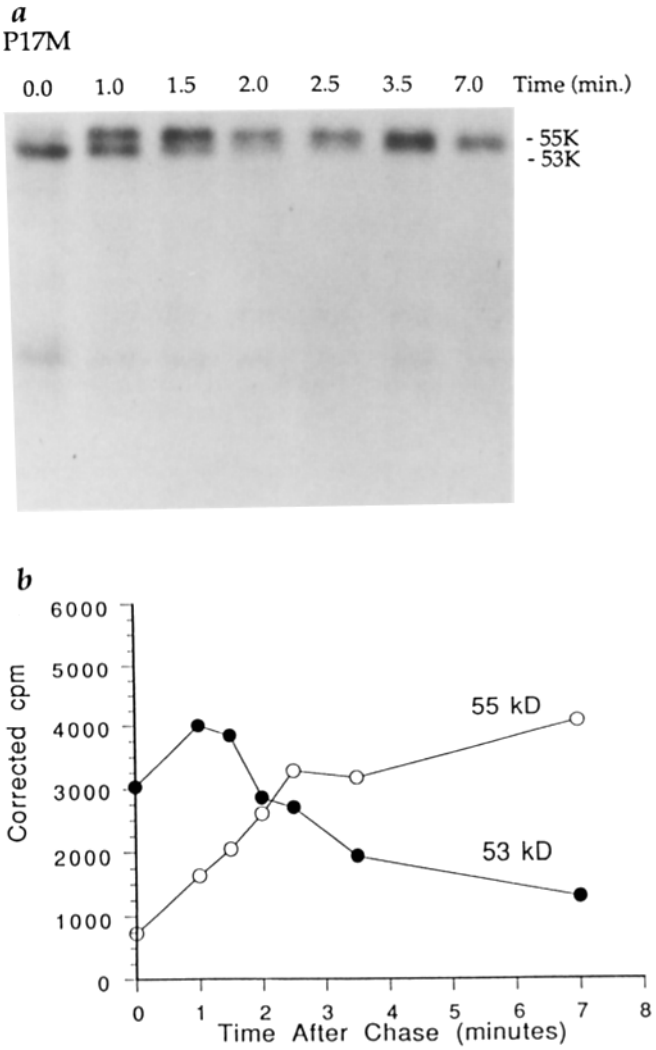

Figure 5. A 53-kD polypeptide is the first AEP precursor detected in a strain carrying the P17M mutation in AEP. It is chased into a 55-kD precursor. (*a*) Immunoprecipitates from a pulse-chases experiment at 33°C. Cells were temperature shifted and labeled as described in Fig. 4. Cell extracts were immunoprecipitated with AEP antisera. (Lanes *1–7*) Immunoprecipitates from samples taken at the times indicated post-chase. The film was exposed for 3 d. (*b*) Graph of the counts in the 53- and 55-kD precursors versus time after the chase. The counts were normalized to compensate for the number of leucines per molecule (32 for the 53-kD precursor and 29 for the 55-kD precursor).

is not translocated in which case it should still contain the signal peptide. Therefore, NH_2-terminal radiosequencing of the 53- and 55-kD AEP precursors was done. Cells were grown at 23°C and double labeled with [^{35}S]methionine

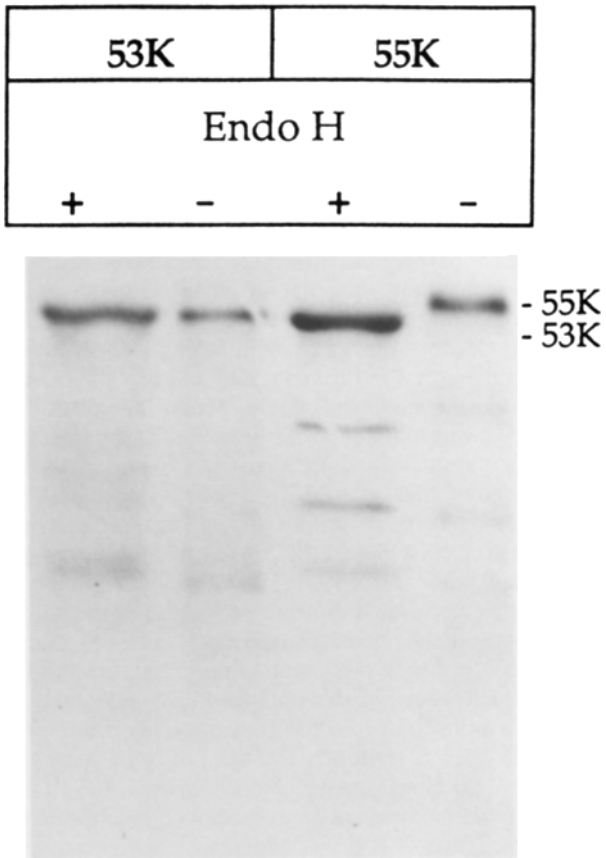

Figure 6. The 53-kD precursor is unglycosylated, while the 55-kD precursor contains ~2 kD of N-linked carbohydrate. Cells were grown at 23°C and labeled for 45 s with [^{3}H]leucine. Immunoprecipitates were digested with endo H and electrophoresed on a 10 to 15% linear gradient SDS-PAGE gel. The lanes contain, from left to right, endo H–digested immunoprecipitate from the 1.5 min sample, immunoprecipitate from the 1.5 min sample, endo H–digested immunoprecipitate from the 10-min sample and immunoprecipitate from the 10-min sample. The positions of the 53- and 55-kD polypeptides are indicated. The film was exposed for 6 d.

Met Lys Leu Ala Thr Ala Phe Thr Ile Leu_{10} Thr Ala Val Leu Ala //Ala Met Leu Ala Ala_{20}

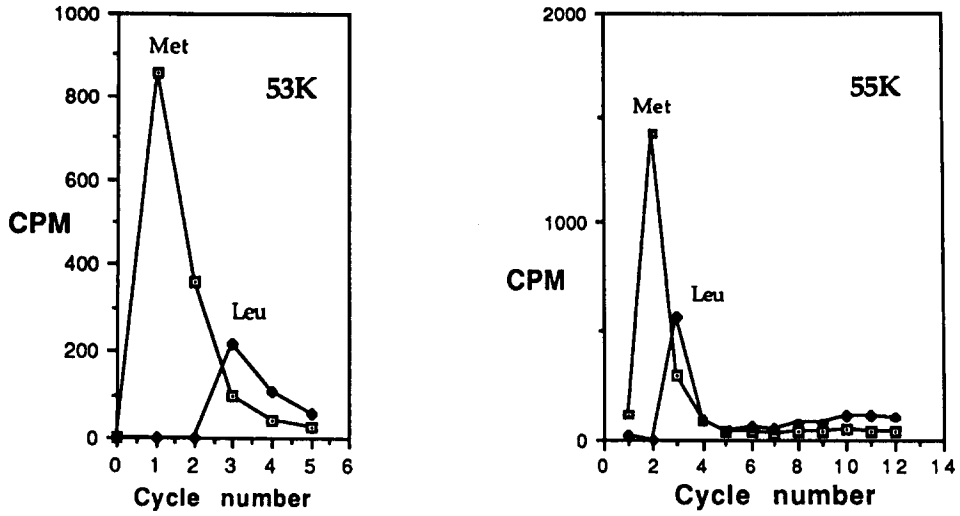

Figure 7. The 55-kD precursor produced in a strain with the P17M mutation contains the signal peptide, and the 55-kD precursor does not. NH_2-terminal radiosequencing of the 53- and 55-kD AEP precursors. Cells were radiolabeled with both [^{35}S]methionine and [^{3}H]leucine for 100 s and chased with both leucine and methionine. Samples were taken as soon as possible and 10 min after the addition of the chase for the 53- and 55-kD precursors, respectively. The cell extracts were immunoprecipitated with AEP antiserum. The immunoprecipitates were run on a 10 to 15% linear gradient SDS-PAGE gels, transferred to Immobilon PVDF membrane, and the membrane bands were cut out and subjected to automated Edman degradation. Results for the 53-kD AEP precursor are on the left, and results for the 55 kD precursor are on the right. The sequence at the top of the figure is the first 20 NH_2-terminal amino acids of the prepro-region of AEP containing the P17M mutation; // indicates the signal peptide cleavage site.

[^{3}H]leucine. After the chase, samples were taken immediately and 10 min after addition of the chase for the 53- and 55-kD precursors, respectively. Radiosequencing of the 53-kD precursor yielded methionine and leucine residues in cycles 1 and 3, respectively (Fig. 7 *a*). This arrangement indicates that the 53-kD precursor begins with the initiator methionine and that it must contain the signal peptide. For the 55-kD precursor, a methionine in cycle 2 and a leucine in cycle 3 were detected indicating that the 55-kD form begins after the signal peptide cleavage site (Fig. 7 *b*). The glycosylation and radiosequencing results both strongly suggest that the 53-kD precursor is not translocated and that the 55-kD precursor is translocated. Thus the P17M AEP molecule appears to be posttranslationally translocated. The fact that the P17M 53-kD untranslocated precursor was readily detected strongly suggests that a wild type untranslocated AEP precursor would also be detectable at 33°C in DY66 (*scrl-1*).

To demonstrate that the P17M 53-kD AEP precursor is untranslocated while the P17M 55-kD AEP precursor is translocated, we performed protease-protection experiments. We labeled intact cells, made spheroplasts, lysed the spheroplasts, and did protease-protection experiments on the lysate. We could demonstrate that both the P17M and wild type 55-kD precursors were protected from proteinase K digestion in the absence of Triton X-100 but not in its presence (data not shown). However, we could not detect the P17M 53-kD AEP precursor even in the control where neither proteinase K nor Triton X-100 was added which suggests that the P17M 53-kD AEP precursor is proteolytically degraded during preparation of cell extracts from spheroplasts.

One explanation for the absence of the P17M 53-kD precursor is that it was being posttranslationally translocated during sample preparation despite addition of sodium azide. In this case, only the 55-kD precursor would be detected. To eliminate this possibility, cells were pulse labeled and taken through the same temperature regime used for spheroplasting and cell lysis. A cell extract was prepared by homogenization with glass beads which should break open both cells and intracellular compartments. Both the P17M 53- and 55-kD AEP precursors were detected, but neither precursor was protected from proteinase K even in the absence of Triton X-100 (data not shown). Therefore, the 53-kD precursor does not appear to be posttranslationally translocated during sample preparation, and this is consistent with in vitro results showing that energy is required for posttranslational translocation (28, 55, 75). We conclude that the P17M 55-kD precursor is in a membrane-bound compartment and that the P17M AEP 53-kD precursor is most likely located outside a membrane-protected compartment where it is more accessible to proteases present in the cell extract.

Detection of the P17M 53-kD untranslocated precursor demonstrates that an untranslocated precursor should be stable enough to be detected in DY66 (*scrl-1*) or wild type. Taken together with the decrease in the levels of the 55-kD AEP precursor in DY66 (*scrl-1*), these results strongly suggest that the *scrl-1* mutation preferentially affects AEP synthesis and not translocation. Based on the models of SRP function, we believe the decrease in AEP synthesis may be due to maintenance of translational arrest (see Discussion).

The scrl-1 Allele Does Not Affect the Levels of P17M AEP Precursors

Results obtained with P17M suggest that full length AEP precursors are being synthesized in the cytoplasm and posttranslationally translocated into the ER. Results from wild type suggest that translocation is co-translational and results with the *scrl-1* mutation suggest that SRP is at least involved in AEP synthesis. The posttranslational translocation of P17M suggests that signal peptide recognition by SRP does not occur, whereas, it seems likely that for the *scrl-1* mutation signal peptide recognition does occur. Therefore, it would be predicted that when the P17M and *scrl-1* mutations were combined in the same strain, the mutated AEP should

Table II. Synthesis after 1 h at 33°C of P17M AEP Precursors in Cells Containing scr1-1 or SCR1

Time after chase (min)	Strain	Number of experiments	(Counts in AEP precursors/Total counts incorporated) × 100%* Mean (SD)		
			53 kD	55 kD	53 kD + 55 kD
0	DY66-P17M (*scr1-1*)	3	0.206 (0.036)	0.124 (0.035)	0.330 (0.059)
0	DY63-P17M (*SCR1*)	2	0.193 (0.013)	0.108 (0.020)	0.301 (0.033)
1	DY66-P17M (*scr1-1*)	2	0.201 (0.033)	0.204 (0.012)	0.439 (0.081)
1	DY63-P17M (*SCR1*)	1	0.195	0.244	0.439
1.5	DY66-P17M (*scr1-1*)	3	0.158 (0.067)	0.284 (0.199)	0.456 (0.257)
1.5	DY63-P17M (*SCR1*)	2	0.165 (0.009)	0.256 (0.061)	0.421 (0.070)

* Cells were grown at 23°C, transferred to 33°C for 1 h, labeled for 45 s with [^{3}H] leucine, and a standard immunoprecipitation was done. Duplicate SDS-PAGE gels were run for twice the normal length of time to increase the separation of the 53- and 55-kD AEP precursors. Bands were detected by fluorography, cut out, and counted.

be posttranslationally translocated, and there should be no translational arrest of P17M synthesis since translational arrest follows and is dependent upon signal peptide recognition.

The P17M allele was substituted for wild type AEP in strains DY63 (*SCR1*) and DY66 (*scr1-1*), and these strains were designated DY63-P17M and DY66-P17M. Pulse-chase immunoprecipitation experiments were done on these strains after a 1 h shift to 33°C. The pattern of immunoprecipitates in both strains was similar to that for a strain with only the P17M mutation; the 53-kD precursor chases into the 55-kD precursor (as in Fig. 5). The counts in the 53- and 55-kD AEP precursors were determined at selected times. There was no evidence for translational arrest of synthesis of either P17M AEP precursor in DY66-P17M compared to DY63-P17M (Table II). Thus, these results are consistent with the original prediction that the defect caused by the P17M mutation occurs earlier in the AEP synthesis/translocation pathway than the defect caused by the *scr1-1* mutation.

Discussion

Translational Arrest?

We have isolated a temperature sensitive mutation in the *SCR1* gene coding for one of the two functional SRP 7S RNAs synthesized in *Y. lipolytica*. The mutation *scr1-1* changes both conserved bases in the conserved sequence -GNAR- in the loop of the domain III stem loop (14). It is not known if either of the base changes alone would cause the phenotype. The *scr1-1* allele could not support growth when integrated at its normal chromosomal location. The plasmid copy number is estimated to be two to three (23) and the increased copy number, perhaps combined with a different transcription rate on the plasmid, probably results in high enough levels of *scr1-1* 7S RNA to compensate for the functional defect(s).

Whether *scr1-1* causes defects in SRP assembly or loss of function of existing SRP molecules remains to be determined. No effect on AEP synthesis was observed at 23°C or at 15 min after the shift to 33°C, while the effects after 1 or 2 h were similar. This implies that existing SRP particles did not rapidly lose functionality. On the other hand 1 h is less than half the doubling time, and if the turnover rate of SRP 7S RNA is low, then defective SRP assembly is a less likely explanation for the effect on AEP synthesis. The fact that the loss of cell viability was not much more rapid than the decrease in AEP synthesis after a shift to 33°C is consistent with the primary defect of the *scr1-1* mutation being the decrease in AEP synthesis (and presumably synthesis of other SRP "dependent" proteins).

Nearly 70% of tetraloops (four nucleotide loops) in rRNAs are either -UNCG- or -GNRA- (25, 77). These two tetraloop sequences also occur in many other RNAs like 7S RNA, the catalytic RNA of RNase P and the self-splicing RNAs (71). The -GNAR- consensus in the stem loop of domain III of the 7S RNA (and specifically the GUAA in *Y. lipolytica*) fits the -GNRA- tetraloop consensus. In addition, the stem loop of domain IV of the *S. pombe* 7S RNA, shown to be important for function (37), also fits the -GNRA- tetraloop consensus. The solution structures of RNA hairpins containing a -GCAA- or -GAAA- tetraloops have been reported recently (32). The hairpin is very compact in shape and has many intramolecular interactions which contribute to its unusual stability (32) and which could provide nucleation sites for correct folding of RNAs (16). The -AUUA- sequence in the *scr1-1* mutation contains two changes from the -GNRA- consensus. It is likely that it affects folding or stability of the 7S RNA, but the possibility of sequence-specific interactions with SRP polypeptides or even the SRP receptor protein cannot be excluded.

A major result of this study is that a mutation in the 7S RNA component of SRP preferentially affects the synthesis of AEP, a secreted protein from *Y. lipolytica*. Although the results with *scr1-1* do not support a role in protein translocation, they constitute in vivo evidence for involvement of SRP with a secreted gene product. The three functions of SRP as defined in vitro are signal recognition, translational arrest, and translocation promotion. A possible explanation of the data which fits current models is that signal recognition and translational arrest were not affected by the *scr1-1* mutation, but that it resulted in decreased ability to release translational arrest after interaction with the SRP receptor or in decreased efficiency of the interaction of the nascent chain/ribosome/SRP complex with the SRP receptor. Since SRP and translational arrest are released after the complex binds to the SRP receptor, this less efficient interaction would lead to the maintenance of translational arrest of AEP synthesis. Translational arrest by SRP has been demonstrated in several in vitro systems (see reference 78), but the only other in vivo evidence for translational arrest is quite indirect (76). We believe that the effect of *scr1-1* mutation on AEP synthesis is

the most direct indication that translational arrest is occurring in vivo. Whether or not it is an essential in vivo function still remains to be determined.

In vitro studies in higher eukaryotes suggested that the loops in domains III and IV of the SRP 7S RNA are bound by Srp19p (64), and that this binding is required for Srp54p binding (64, 65). However, recent results suggest that domain III may interfere with Srp54p binding in the absence of Srp19p and that after Srp19p binding there is a conformational change in the 7S RNA so that Srp54p now can bind to the stem loop in domain IV (54, 80). Since Srp54p interacts with the signal peptide (34), we originally expected *scr1-1* to decrease the affinity of SRP for the signal peptide resulting in accumulation of an untranslocated AEP precursor. Instead, our results suggest that the mutated loop might affect the conformation or binding of Srp68p, which is believed to interact with the SRP receptor (64–66), or that SRP 7S RNA interacts directly with SRP receptor.

The total counts incorporated and the ratio of Con A bound counts to total counts varied substantially from experiment to experiment (Table I). However, within an experiment the comparison of the ratios of bound/total counts was quite consistent with values for DY66 (*scr1-1*) being 67–77% of those for DY63 (*SCR1*) for an average decrease of 27%. This value is somewhat of an underestimate as some labeled glycoproteins are cytoplasmic or nuclear (29). However, unless they are a large percentage of the total glycoproteins, the decrease in synthesis for secreted proteins determined in the Con A experiment is significantly less than the decrease in AEP synthesis. This suggests that biosynthesis of other secretory proteins is not as severely affected by the *scr1-1* defect as is AEP biosynthesis. This is consistent with translational arrest by SRP not necessarily being complete (78) and with the degree of arrest depending on the specific signal peptide.

The decrease in secreted AEP synthesized in DY66 (*scr1-1*) compared to DY63 (*SCR1*) was also about threefold less than for the 55-kD AEP precursor. Calculated based on the percentage of total counts incorporated found in secreted AEP, the decrease averaged 22% for the last three samples in Fig. 4 *b*. The reason for this difference is unknown. The use of immunoprecipitation to measure levels of the 55-kD AEP precursor, a transient intermediate, may overestimate the decrease in AEP synthesis. If translational arrest results in a range of less than full-length precursors, they might be less efficiently precipitated and they might not be detected because they would be spread out over the gel lane. Early in the chase, more labeled partially completed precursor molecules would be expected in DY66 (*scr1-1*) than in DY63 (*SCR1*) because of the maintenance of translational arrest. However, eventually arrest would be released and this previously undetected label would ultimately accumulate in secreted AEP.

Co- and Posttranslational Translocation

Another significant result of this study is the posttranslational translocation of the mutated P17M AEP. Although posttranslational protein translocation has been demonstrated both in vivo and in vitro for procaryotes (41) and *S. cerevisiae* (2, 10, 20, 27, 28, 38, 42, 55, 57, 67, 70, 75), *Y. lipolytica* is the most evolutionarily advanced organism in which in vivo posttranslational translocation has been shown to occur. *Y. lipolytica* is dimorphic, growing as either yeast-like or filamentous forms, and in many ways such as the organization of its rRNA genes (17, 72) it appears more closely related to the filamentous fungi than to other yeast genera. Based on 18S rRNA sequences, the evolutionary distance between *Y. lipolytica* and *S. cerevisiae* (5) is comparable or greater than that between *S. cerevisiae* and *S. pombe* (W. Weisburg, personal communication). A comparison of snRNAs in various yeasts revealed that the sizes of the *Y. lipolytica* snRNAs were much closer to those for human than were the snRNAs from *S. cerevisiae* (53). By several criteria the *Y. lipolytica* SRP 7S RNA is more higher eucaryotic-like than the *S. cerevisiae* homologue. The *Y. lipolytica* SRP 7S RNAs are closer in size and seemingly secondary structure, 270 nucleotides (30, 46) versus 300 for human (74) and 519 for the *S. cerevisiae SCR1* gene product (22). In *Y. lipolytica* the *SCR* genes are essential for growth (31)) and not just important as in *S. cerevisiae* (22). Finally, higher eucaryotes have multiple transcribed SRP 7S RNAs (81), and *Y. lipolytica* is the only genetically tractable lower eucaryote having more than one functional SRP 7S RNA.

The conclusion that the P17M AEP is translocated posttranslationally was based on several findings. The kinetics of the pulse-chase experiments fit a precursor-product relationship for the 53- and 55-kD precursors. An untranslocated precursor would be expected to contain the signal peptide and to lack N-linked carbohydrate as was found for the P17M 53-kD AEP precursor. A translocated precursor would be expected to lack the signal peptide and to contain N-linked carbohydrate as was found for the P17M 55-kD AEP precursor. The protease-protection experiments demonstrate that the P17M 55-kD AEP precursor is located in a membrane-bound compartment and are consistent with a cytoplasmic location for the P17M 53-kD AEP precursor.

The results with P17M in a wild type background and with DY66-P17M suggest that the signal peptide was not recognized by SRP. The P17M mutation may affect the conformation or accessibility of the signal peptide. In vitro experiments with preprolactin suggest that subtle sequence changes beyond the signal cleavage site could affect signal peptide function, and co-translational translocation was less efficient in the preprolactin mutants (4). However, translational arrest by SRP in vitro in the absence of membranes did not seem to be affected (4).

The presence of the 55-kD AEP precursor in the earliest time point samples raised the possibility that some translocation of P17M AEP precursors was occurring co-translationally. If this were the case then the level of 55-kD synthesis in DY66-P17M would be expected to be lower than in DY63-P17M. However, no significant difference was found suggesting that all or nearly all the 55-kD AEP precursor was translocated posttranslationally. If the P17M precursor does not interact with SRP, then how it is targeted to the ER membrane and whether or not it uses the same translocation machinery as used for SRP-mediated co-translational translocation are open questions. It should be noted that the translocation of P17M AEP is kinetically quite inefficient compared to co-translocational translocation of wild type AEP.

The results obtained with the mutated P17M AEP are not inconsistent with co-translational translocation (with SRP at least involved in AEP synthesis) being the major pathway for

AEP translocation in wild type cells. In fact, the demonstration that an untranslocated AEP precursor can be detected in the mutant strengthens the conclusion (based on the absence of untranslocated precursors even after labeling times as short as 30 s) that translocation is co-translational in the wild type. Recently in vitro evidence for posttranslational and SRP-mediated co-translational translocation was obtained for dog pancreas microsomal membranes (61), and in vivo evidence for involvement of SRP homologues in protein translocation in *S. cerevisiae* may be forthcoming (48). However, assuming that SRP is involved not only in synthesis but also in translocation of AEP, then AEP would be the first protein for which there would be in vivo evidence for both posttranslational and SRP-mediated co-translational translocation. The AEP results are consistent with a recent *E. coli* model where the co-translational pathway is mediated by SRP-like ribonucleoprotein and the posttranslational pathway is a salvage pathway (50).

We thank C. Gaillardin and P. Fournier for *ARS18*, *LYS5*, and *SCR2*, J. Gardner at the University of California at Davis, Protein Structure Laboratory for NH_2-terminal sequencing, J. DeZeeuw for the *T. harzianum* lytic enzyme, and C. Enderlin, C. Gaillardin, and M. Poritz for helpful discussions.

This work was supported by The National Science Foundation and the California Agricultural Experiment Station.

Received for publication 19 June 1991 and in revised form 16 October 1991.

Note Added in Proof. Recently, Hann and Walter (1991. *Cell.* 67:131–144) and Amaya and Nakano (1991. *FEBS [Fed. Eur. Biochem. Soc.] Lett.* 283:325–328) reported that depletion of the SRP 54-kD homologue from *S. cerevisiae* affected translocation of some proteins.

References

1. Amaya, Y., A. Nakano, K. Ito, and M. Mori. 1990. Isolation of a yeast gene, *SRH1*, that encodes a homologue of the 54K subunit of mammalian signal recognition particle. *J. Biochem.* 107:457–463.
2. Allison, D. S., and E. T. Young. 1989. Mutations in the signal sequence of prepro-α-factor inhibit both translocation into the endoplasmic reticulum and processing by signal peptidase in yeast cells. *Mol. Cell. Biol.* 9:4977–4985.
3. Andreazzoli, M., and S. A. Gerbi. 1991. changes in 7SL RNA conformation during the recognition particle cycle. *EMBO (Eur. Mol. Biol. Organ.) J.* 10:767–777.
4. Andrews, D. A., E. Perara, C. Lesser, and V. R. Lingappa. 1988. Sequences beyond the cleavage site influence signal peptide function. *J. Biol. Chem.* 263:15791–15798.
5. Barns, S. M., D. J. Lane, M. L. Sogin, C. Bibeau, and W. G. Weisburg. 1991. Evolutionary relationships among pathogenic *Candida* species and relatives. *J. Bacteriol.* 173:2250–2255.
6. Barth, G., and H. Weber. 1984. Improved conditions for mating of the yeast *Saccharomycopsis lipolytica*. *Z. Allg. Mikrobiol.* 24:403–405.
7. Bassford, P., J. Beckwith, K. Ito, C. Kumamoto, S. Mizushima, D. Oliver, L. Randall, T. Silhavy, P. C. Tai, and B. Wickner. 1991. The primary pathway of protein export in *E. coli*. *Cell.* 65:367–368.
8. Beckwith, J. 1991. "Sequence-gazing?" *Science (Wash. DC).* 251:1161.
9. Biggin, M. D., T. J. Gibson, and G. F. Hong. 1983. Buffer gradient gels and ^{35}S label as an aid to rapid DNA sequence determination. *Proc. Natl. Acad. Sci. USA.* 80:3963–3965.
10. Blachly-Dyson, E., and T. H. Stevens. 1987. Yeast carboxypeptidase Y can be translocated and glycosylated without its amino-terminal signal sequence. *J. Cell Biol.* 104:1183–1191.
11. Boeke, J. D., J. Truehart, G. Natsoulis, and G. R. Fink. 1987. 5-Fluoroorotic acid as a selective agent in yeast molecular genetics. *Methods Enzymol.* 154:164–175.
12. Breenwald, P., X. Liao, K. Holm, G. Porter, and J. A. Wise. 1988. Identification of an essential *Schizosaccharomyces pombe* RNA homologous to the 7SL component of signal recognition particle. *Mol. Cell. Biol.* 8:1580–1590.
13. Brown, S. 1991. Genes for 7S RNAs can replace the gene for 4.5S RNA in growth of *Escherichia coli*. *J. Bacteriol.* 173:1835–1837.
14. Campos, N., J. Palau, and C. Zwieb. 1989. Diversity of 7SL RNA from the signal recognition particle of maize endosperm. *Nucleic Acids Res.* 17:1573–1588.
15. Chen, E. Y., and P. H. Seeburg. 1985. Supercoil sequencing: a fast and simple method for screening plasmid DNA. *DNA* 4:165–170.
16. Cheong, C. G. Varani, and I. Tinoco, Jr. 1990. Solution structure of an unusually stable RNA hairpin 5′ GGAC(UUCG)GUCC. *Nature (Lond.).* 346:680–682.
17. Clare, J. D., L. S. Davidow, D. C. J. Gardner, and S. G. Oliver. 1986. Cloning and characterization of the ribosomal RNA genes of the dimorphic yeast, *Yarrowia lipolytica*. *Curr. Genet.* 10:449–452.
18. Davidow, L. S., F. S. Kaczmarek, J. R. DeZeeuw, S. W. Conlon, M. R. Lauth, D. A. Pereira, and A. E. Franke. 1987. The *Yarrowia lipolytica LEU2* gene. *Curr. Genet.* 11:377–383.
19. Deshaies, R. J., and R. Schekman. 1987. A yeast mutant defective at an early stage in import of secretory protein precursors into the endoplasmic reticulum. *J. Cell Biol.* 105:633–645.
20. Deshaies, R. J., B. D. Koch, M. Werner-Washburne, E. A. Craig, and R. Schekman. 1988. A subfamily of stress proteins facilitates translocation of secretory and mitochondrial precursor polypeptides. *Nature (Lond.).* 332:800–805.
21. Fabre, E., J. M. Nicaud, M. C. Lopez, and C. Gaillardin. 1991. Role of the proregion in the production and secretion of the *Yarrowia lipolytica* alkaline extracellular protease. *J. Biol. Chem.* 266:3782–3790.
22. Felici, F., G. Cesareni, and J. M. X. Hughes. 1989. The most abundant small cytoplasmic RNA of *Saccharomyces cerevisiae* has an important function required for normal cell growth. *Mol. Cell. Biol.* 9:3260–3268.
23. Fournier, P., L. Guyaneux, M. Chasles, and C. Gaillardin. 1991. Scarcity of *ars* sequences isolated in a morphogenesis mutant of the yeast *Yarrowia lipolytica*. *Yeast.* 7:25–36.
24. Geisselsoder, J., F. Witney, and P. Yuckenberg. 1987. Efficient site-directed *in vitro* mutagenesis. *Biotechniques.* 5:786–791.
25. Gutell, R. R., and G. E. Fox. 1988. A compilation of large subunit RNA sequences presented in structural format. *Nucleic Acids Res.* 16(suppl): r175–r269.
26. Hann, B. C., M. A. Poritz, and P. Walter. 1989. *Saccharomyces cerevisiae* and *Schizosaccharomyces pombe* contain a homologue to the 54-kD subunit of the signal recognition particle that in *S. cerevisiae* is essential for growth. *J. Cell Biol.* 109:3223–3230.
27. Hansen, W., and P. Walter. 1988. Prepro-carboxypeptidase Y and a truncated form of pre-invertase, but not full-length pre-invertase, can be post-translationally translocated across microsomal vesicle membranes from *Saccharomyces cerevisiae*. *J. Cell Biol.* 106:1075–1081.
28. Hansen, W., P. D. Garcia, and P. Walter. 1986. *In vitro* translocation across the yeast endoplasmic reticulum: ATP-dependent posttranslational translocation of the prepro-α-factor. *Cell.* 45:397–406.
29. Hart, G. W., R.S. Haltiwanger, G. D. Holt, and W. G. Kelly. 1989. Glycosylation in the nucleus and the cytoplasm. *Ann. Rev. Biochem.* 58:841–874.
30. He, G., J. M. Beckerich, V. Ribes, D. Tollervey, and C. M. Gaillardin. 1989. Two genes encode 7SL RNAs in the yeast *Yarrowia lipolytica*. *Curr. Genet.* 16:347–350.
31. He, F., D. Yaver, J. M. Beckerich, D. Ogrydziak, and C. Gaillardin. 1990. The yeast *Yarrowia lipolytica* has two, functional, signal recognition particle 7S RNA genes. *Curr. Genet.* 17:289–292.
32. Heus, H. A., and A. Pardi. 1991. Structural features that give rise to the unusual stability of RNA hairpins containing GNRA loops. *Science (Wash. DC).* 253:191–194.
33. Hunkapiller, M. W., E. Lujan, F. Ostrander, and L. E. Hood. 1983. Isolation of microgram quantities of proteins from polyacrylamide gels for amino acid sequence analysis. *Methods Enzymol.* 91:227–236.
34. Krieg, U. C., P. Walter, and A. E. Johnson. 1986. Photocrosslinking of the signal sequence of nascent preprolactin to the 54-kilodalton polypeptide of the signal recognition particle. *Proc. Natl. Acad. Sci. USA.* 83: 8604–8608.
35. Kunkel, T. A., J. D. Roberts, and R. A. Zakour. 1987. Rapid and efficient site-specific mutagenesis without phenotypic selection. *Methods Enzymol.* 154:367–382.
36. Lauffer, L., P. D. Garcia, R. N. Harkins, L. Coussens, A. Ullrich, and P. Walter. Topology of signal recognition particle receptor in endoplasmic reticulum membrane. *Nature (Lond.).* 318:334–338.
37. Liao, X., P. Brennwald, and J. A. Wise. 1989. Genetic analysis of *Schizosaccharomyces pombe* 7SL RNA: a structural motif that includes a conserved tetranucleotide loop is important for function. *Proc. Natl. Acad. Sci. USA.* 86:4137–4141.
38. Lolle, S. J., and H. Bussey. 1986. *In vivo* evidence for posttranslational translocation and signal cleavage of the killer preprotoxin of *Saccharomyces cerevisiae*. *Mol. Cell. Biol.* 6:4274–4280.
39. Matoba, S., and D. M. Ogrydziak. 1989. A novel location for dipeptidyl aminopeptidase processing sites in the alkaline extracellular protease of *Yarrowia lipolytica*. *J. Biol. Chem.* 264:6037–6043.
40. Matoba, S., J. Fukayama, R. A. Wing, and D. M. Ogrydziak. 1988. Intracellular precursors and secretion of alkaline extracellular protease of *Yarrowia lipolytica*. *Mol. Cell. Biol.* 8:4904–4916.
41. Model, P., and M. Russel. 1990. Prokaryotic secretion. *Cell.* 61:739–741.
42. Ngsee, J., W. Hansen, P. Walter, and M. Smith. 1989. Cassette mutagenic

analysis of the yeast invertase signal peptide: effects on protein translocation. *Mol. Cell. Biol.* 9:3400–3410.
43. Ogrydziak, D. M., and S. J. Scharf. 1982. Alkaline extracellular protease produced by *Saccharomyces lipolytica* CX161-1B. *J. Gen. Microbiol.* 128:1225–1234.
44. Ogrydziak, D. M., J. Bassel, R. Contopoulou, and R. Mortimer. 1978. Development of genetic techniques and the genetic map of the yeast *Saccharomycopsis lipolytica*. *Mol. Gen. Genet.* 163:229–239.
45. Osawa, T., and T. Tsuji. 1987. Fractionation and structural assessment of oligosaccharides and glycopeptides by use of immobilized lectins. *Ann. Rev. Biochem.* 56:21–42.
46. Poritz, M. A., V. Siegel, W. Hansen, and P. Walter. 1988. Small ribonucleoproteins in *Schizosaccharomyces pombe* and *Yarrowia lipolytica* homologous to signal recognition particle. *Proc. Natl. Acad. Sci. USA.* 85: 4315–4319.
47. Poritz, M. A., H. D. Bernstein, K. Strub, D. Zopf, H. Wilhelm, and P. Walter. 1990. An *E. coli* ribonucleoprotein containing 4.5S RNA resembles mammalian signal recognition particle. *Science (Wash. DC).* 250: 1111–1117.
48. Poritz, M. A., H. D. Bernstein, and P. Walter. 1991. "Sequence-gazing?"-response. *Science (Wash. DC).* 251:1161–1162.
49. Rapoport, T. A. 1990. Protein transport across the ER membrane. *Trends Biochem. Sci.* 15:355–358.
50. Rapoport, T. A. 1991. A bacterium catches up. *Nature (Lond.).* 349: 107–108.
51. Ribes, V., P. Dehoux, and D. Tollervey. 1988. 7SL RNA from *Schizosaccharomyces pombe* is encoded by a single copy essential gene. *EMBO (Eur. Mol. Biol. Organ.) J.* 7:231–237.
52. Ribes, V., K. Romisch, A. Giner, B. Dobberstein, and D. Tollervey. 1990. *E. coli* 4.5S RNA is part of a ribonucleoprotein particle that has properties related to signal recognition particle. *Cell.* 63:591–600.
53. Roiha, H., E. O. Shuster, D. A. Brow, and C. Guthrie. 1989. snRNAs from budding yeasts: phylogenetic comparisons reveal extensive size variation. *Gene.* 82:137–144.
54. Romisch, K., J. Webb, K. Lingelbach, H. Gausepohl, and B. Dobberstein. 1990. The 54-kD protein of signal recognition particle contains a methionine-rich RNA binding domain. *J. Cell Biol.* 111:1793–1802.
55. Rothblatt, J. A., and D. I. Meyer. 1986. Secretion in yeast: reconstitution of the translocation and glycosylation of α-factor and invertase in a homologous cell-free system. *Cell.* 44:619–628.
56. Rothblatt, J., and R. Schekman. 1989. A hitchhiker's guide to analysis of the secretory pathway in yeast. *Methods Cell Biol.* 32:3–36.
57. Rothblatt, J. A., R. J. Deshaies, S. L. Sanders, G. Daum, and R. Schekman. 1989. Multiple genes are required for proper insertion of secretory proteins into the endoplasmic reticulum in yeast. *J. Cell Biol.* 109: 2641–2652.
58. Rothstein, R. J. 1983. One-step gene disruption in yeast. *Methods Enzymol.* 101:202–211.
59. Sambrook, J., E. F. Fritsch, and T. Maniatis. 1989. Molecular Cloning: A Laboratory Manual, 2nd ed. Cold Spring Harbor Laboratory, Cold Spring Harbor, NY. A.9–A.12 and 7.43–7.45.
60. Sanger, F., S. Nicklen, and A. R. Coulson. 1977. DNA sequencing with chain-terminating inhibitors. *Proc. Natl. Acad. Sci. USA.* 74:5463–5467.
61. Schlenstedt, G., G. H. Gudmundsson, H. G. Boman, and R. Zimmerman. 1990. A large presecretory protein translocates both cotranslationally, using signal recognition particle and ribosome, and post-translationally, without these ribonucleoparticles, when synthesized in the presence of mammalian microsomes. *J. Biol. Chem.* 265:13960–13968.
62. Sherman, F., G. R. Fink, and J. B. Hicks. 1986. Laboratory Course Manual for Methods in Yeast Genetics. Cold Spring Harbor Laboratory, Cold Spring Harbor, NY. 186 pp.
63. Siegel, V., and P. Walter. 1985. Elongation arrest is not a prerequisite for secretory protein translocation across the microsomal membrane. *J. Cell Biol.* 100:1913–1921.
64. Siegel, V., and P. Walter. 1988. Binding sites of the 19-kDa and 68/72-kDa signal recognition particle (SRP) proteins on SRP RNA as determined by protein-RNA "footprinting." *Proc. Natl. Acad. Sci. USA.* 85:1801–1805.
65. Siegel, V., and P. Walter. 1988. Each of the activities of signal recognition particle (SRP) is contained within a distinct domain: analysis of biochemical mutants of SRP. *Cell.* 52:39–49.
66. Siegel, V., and P. Walter. 1988. Functional dissection of the signal recognition particle. *Trends Biochem. Sci.* 13:314–316.
67. Silve, S., M. Monod, A. Hinnen, and R. H. Haguenauer-Tsapis. 1987. The yeast acid phosphatase can enter the secretory pathway without its N-terminal signal sequence. *Mol. Cell Biol.* 7:3306–3314.
68. Tabor, S., and C. C. Richardson. 1987. DNA sequence analysis with modified bacteriophage T7 DNA polymerase. *Proc. Natl. Acad. Sci. USA.* 84:4767–4771.
69. Towbin, H., T. Staehlin, and J. Gordon. 1979. Electrophoretic transfer of proteins from polyacrylamide gels to nitrocellulose sheets: procedures and some applications. *Proc. Natl. Acad. Sci. USA.* 76:4350–4354.
70. Toyn, J., A. R. Hibbs, P. Sanz, J. Crowe, and D. I. Meyer. 1988. *In vivo* and *in vitro* analysis of *ptl1*, a yeast *ts* mutant with a membrane-associated defect in protein translocation. *EMBO (Eur. Mol. Biol. Organ.) J.* 7: 4347–4353.
71. Uhlenbeck, O. C. 1990. Tetraloops and RNA folding. *Nature (Lond.).* 346: 613–614.
72. Van Heerikhoizen, H., A. Ykema, J. Klootwijk, C. Gaillardin, C. Ballas, and P. Fournier. 1985. Heterogeneity in the ribosomal RNA genes of the yeast *Yarrowia lipolytica*: cloning and analysis of two sizes of repeats. *Gene.* 39:213–222.
73. Walter, P., and G. Blobel. 1983. Disassembly and reconstitution of signal recognition particle. *Cell.* 34:525–533.
74. Walter, P., and V. R. Lingappa. 1986. Mechanism of protein translocation across the endoplasmic reticulum membrane. *Ann. Rev. Cell Biol.* 2:499–516.
75. Waters, M. G., and G. Blobel. 1986. Secretory protein translocation in yeast cell-free system can occur post-translationally and requires ATP hydrolysis. *J. Cell Biol.* 102:1543–1550.
76. Welsh, M., N. Scherberg, R. Gilmore, and D. F. Steiner. 1986. Translational control of insulin biosynthesis. Evidence for regulation of elongation, initiation and signal-recognition-particle-mediated translational arrest by glucose. *Biochem. J.* 235:459–467.
77. Woese, C. R., R. Gutell, R. Gupta, and N. F. Noller. 1983. Detailed analysis of the higher-order structure of 16S-like ribosomal ribonucleic acids. *Microbiol. Rev.* 47:621–669.
78. Wolin, S. L., and P. Walter. 1989. Signal recognition particle mediates a transient elongation arrest of preprolactin in reticulocyte lysate. *J. Cell Biol.* 109:2617–2622.
79. Xuan, J.-W., P. Fournier, and C. Gaillardin. 1988. Cloning of the *LYS5* gene encoding saccharopine dehydrogenase from the yeast *Yarrowia lipolytica* by target integration. *Curr. Genet.* 14:15–21.
80. Zopf, D., H. D. Bernstein, A. E. Johnson, and P. Walter. 1990. The methionine-rich domain of the 54 kd protein subunit of the signal recognition particle contains an RNA binding site and can be crosslinked to a signal sequence. *EMBO (Eur. Mol. Biol. Organ.) J.* 9:4511–4517.
81. Zwieb, C. 1989. Structure and function of signal recognition particle RNA. *Prog. Nucleic Acid Res. Mol. Biol.* 37:207–234.